Environmental Research Letters

LETTER

Global change accelerates carbon assimilation by a wetland ecosystem engineer

Joshua S Caplan[1,2], **Rachel N Hager**[1,2,3], **J Patrick Megonigal**[2] **and Thomas J Mozdzer**[1,2]

[1] Department of Biology, Bryn Mawr College, 101 North Merion Avenue, Bryn Mawr, PA 19010, USA
[2] Smithsonian Environmental Research Center, 647 Contees Wharf Road, Edgewater, MD 21037, USA
[3] Ecology Center and Department of Watershed Sciences, Utah State University, 5210 Old Main Hill, Logan, UT 84322, USA

E-mail: jcaplan@mail.com

Keywords: coastal wetland, elevated CO_2, eutrophication, global change, *Phragmites australis* (common reed), tidal saltmarsh, primary productivity

Supplementary material for this article is available online

OPEN ACCESS

RECEIVED
27 May 2015

REVISED
14 October 2015

ACCEPTED FOR PUBLICATION
19 October 2015

PUBLISHED
16 November 2015

Abstract

The primary productivity of coastal wetlands is changing dramatically in response to rising atmospheric carbon dioxide (CO_2) concentrations, nitrogen (N) enrichment, and invasions by novel species, potentially altering their ecosystem services and resilience to sea level rise. In order to determine how these interacting global change factors will affect coastal wetland productivity, we quantified growing-season carbon assimilation (≈gross primary productivity, or GPP) and carbon retained in living plant biomass (≈net primary productivity, or NPP) of North American mid-Atlantic saltmarshes invaded by *Phragmites australis* (common reed) under four treatment conditions: two levels of CO_2 (ambient and +300 ppm) crossed with two levels of N (0 and 25 g N added m^{-2} yr^{-1}). For GPP, we combined descriptions of canopy structure and leaf-level photosynthesis in a simulation model, using empirical data from an open-top chamber field study. Under ambient CO_2 and low N loading (i.e., the Control), we determined GPP to be 1.66 ± 0.05 kg C m^{-2} yr^{-1} at a typical *Phragmites* stand density. Individually, elevated CO_2 and N enrichment increased GPP by 44 and 60%, respectively. Changes under N enrichment came largely from stimulation to carbon assimilation early and late in the growing season, while changes from CO_2 came from stimulation during the early and mid-growing season. In combination, elevated CO_2 and N enrichment increased GPP by 95% over the Control, yielding 3.24 ± 0.08 kg C m^{-2} yr^{-1}. We used biomass data to calculate NPP, and determined that it represented 44%–60% of GPP, with global change conditions decreasing carbon retention compared to the Control. Our results indicate that *Phragmites* invasions in eutrophied saltmarshes are driven, in part, by extended phenology yielding 3.1× greater NPP than native marsh. Further, we can expect elevated CO_2 to amplify *Phragmites* productivity throughout the growing season, with potential implications including accelerated spread and greater carbon storage belowground.

1. Introduction

Global change is altering the fundamental ecological processes that control coastal wetland productivity, and is thereby altering ecosystem processes such as soil accretion, elevation gain, and carbon sequestration [1, 2]. Global change affects primary productivity, for example, by altering photosynthetic rates, temporal patterns of growth, allocation to above- versus below-ground organs, and plant community composition [3]. Such changes have the potential to alter the resilience of tidal wetlands to sea level rise, with consequences for ecosystem services like providing wildlife habitat and protecting coasts from storm surges [4].

The productivity response of marsh ecosystems to global change is highly context specific, with the response to rising atmospheric carbon dioxide (CO_2)

concentrations dependent on local abiotic conditions such as nitrogen (N) loading, salinity, and functional traits of the biotic community, including the dominant photosynthetic pathway [5–7]. Although research on native plant communities has provided strong insights into the relationships of rising CO_2, N loading, and biotic change in coastal wetlands [6, 8], biological invaders are re-engineering coastal ecosystems, thus modifying how global change factors influence ecosystem productivity, resilience to sea level rise, and provisioning of ecosystem services [9, 10].

Invasive plant species and genotypes not only respond to environmental change but also amplify or fundamentally alter ecological processes through novel traits or feedbacks [11], and can therefore be considered a form of global change themselves [12]. Several highly successful plant invasions have proceeded through this form of ecosystem re-engineering; the most prominent case in North American coastal wetlands is that of *Phragmites australis* (hereafter *Phragmites*) or common reed. *Phragmites* is a clonal C_3 grass that grows in fresh to polyhaline wetlands throughout the world [13]. Although there are many genetic lineages of *Phragmites* globally, one haplotype (designated M) is highly invasive in North America, where it was introduced from Eurasia in the 1800s [14]. Several *Phragmites* lineages, including haplotype M, are known to have particularly strong trait responses to elevated CO_2, temperature, and N conditions, such as increased light-saturated photosynthetic rates, relative growth rates, and stand densities [15–17]. However, experiments evaluating *Phragmites* traits and their responses to global change have been short-term and have used young, containerized plants [15–19], thus limiting their ability to provide insight into ecosystem-level processes. Quantification of carbon fluxes and storage in *Phragmites*-dominated marshes, for example, requires data from mature clones growing in the field. Such quantification would be useful for carefully evaluating if and how *Phragmites* will alter rates of soil elevation gain under future environmental conditions. Some have suggested that the negative effects of *Phragmites* invasion be weighed against its potential to enable some coastal wetlands to keep pace with accelerating rates of sea level rise [20].

Relatively few data sets describe variation in carbon assimilation under expected future CO_2 conditions at timescales necessary to provide insight into the influence of intra-annual temporal patterns on annual productivity. However, growth and senescence phenology can strongly influence annual productivity, e.g., by moderating canopy structure [21, 22] or the duration of the growing period [23–25]. Further, these phenological changes are influenced by global change factors such as CO_2, N, and temperature [23, 26, 27]. Much of the research on plant productivity responses to global change is based on plant biomass measurements, with data collected one to a few times annually [6, 28]. A lack of fine-scale, temporally explicit data on carbon assimilation rates under predicted future conditions limits our ability to understand and model the effects of global change on coastal wetlands.

Although CO_2, N, and other global change factors can be manipulated in the field, quantifying carbon fluxes at a high temporal frequency in concert with such experiments poses methodological challenges. Eddy covariance generates high frequency data and has been used successfully in coastal wetlands [29–31], but fumigation with CO_2 disrupts the CO_2 gradients that are the basis of the technique. Measurements of carbon assimilation can be made with flux chambers [32, 33], but collecting data at a sufficient interval to capture variation in solar radiation is prohibitively difficult; this is especially true for large-stature species such as *Phragmites* (heights reach 4 m). Modeling can be used to overcome these challenges, though accurate modeling under global change conditions requires vegetative responses to these conditions to be determined and represented. At large spatial scales, this has been achieved by coupling models of carbon cycling and climate processes, and running these models under various emissions scenarios [34]. At the smaller scales relevant to determining the influence of plant community composition on productivity, modeling has enabled leaf-level carbon fluxes to be extended to the stand scale [24, 35, 36]. Empirical data from manipulative global change field experiments can provide the relationships and parameters needed to accurately represent differences in plant physiology and canopy structure in such models.

We present here a quantification of gross primary productivity (GPP) by *Phragmites* in a North American mid-Atlantic Coast wetland that is finely temporally scaled (hourly to daily) and was derived from a combination of experimentation and modeling. Using data and relationships derived from a new, manipulative field experiment on the Chesapeake Bay, we simulated *Phragmites* growth, canopy structure, and carbon assimilation under factorial combinations of atmospheric CO_2 and N loading. Although *Phragmites* stand dynamics have been modeled successfully several times before [37–42], these efforts did not consider the effects of global change on model parameters, and most focused on aboveground productivity. We specifically determined how global change will alter the magnitude of carbon assimilation by *Phragmites* tidal marshes at the annual timescale (GPP_a) as well as temporal patterns of carbon assimilation through the growing season. We also estimated annual net primary productivity (NPP_a) of *Phragmites* marshes, and used these values to constrain carbon use efficiency (CUE), i.e., the fraction of GPP_a retained, under the global change treatments considered. Finally, we compared the stimulation effects of *Phragmites* marshes (based on GPP_a and NPP_a) to each other and to those of native marshes (based on NPP_a). We expected *Phragmites* to increase GPP_a and NPP_a in response to both elevated CO_2 and N enrichment, but to experience the

greatest productivity stimulation under the combined treatment. Further, we expected *Phragmites* to increase its CUE under all global change conditions and to exhibit stronger stimulation effects than the native community.

2. Methods

2.1. Field experiment

The field experiment was established in a brackish tidal marsh within the Smithsonian Global Change Research Wetland (Kirpatrick Marsh; 38.8742° N, 76.5474° W) in Edgewater, Maryland, USA. Salinity at the site varies from 4–15 ppt (mean = 10 ppt) and the mean tidal range is 44 cm. The high-marsh platform is 40–60 cm above the mean low water level, and soils are predominantly organic (>80%) to 5 m depth. Mean daily air temperatures range from −4 to 31 °C and mean annual precipitation is 108 cm. The native plant community is dominated by the C_3 sedge *Schoenoplectus americanus* (formerly *Scirpus americanus* and *S. olneyi*) and the C_4 grasses *Spartina patens* and *Distichlis spicata*. A single stand of *Phragmites* was documented in 1972 [43], whereas it now covers approximately 25% of the site.

Twelve open-top chambers (OTCs; 1.25 × 2.5 × 4.4 m) were installed at the leading edge of an expanding *Phragmites* stand in 2011. During the 2011–2013 growing seasons (May through October) half of the OTCs were fumigated with air approximately 300 ppm CO_2 above ambient levels (denoted eCO_2), while the remaining chambers were fumigated with unamended air. This CO_2 level is representative of those predicted for year 2100 under a moderate rise in global atmospheric CO_2 (e.g., scenario RCP6 [44]), and has been used in other experiments at the site [2, 5]. Three OTCs of each CO_2 treatment type received 25 g N m^{-2} yr^{-1} (denoted N_{enr}), which was applied monthly during the growing season as dissolved NH_4Cl (5 g N m^{-2} per month). This enrichment level represents moderate N loading in wetlands of the Chesapeake Bay [45] and has been used in an experiment in the native community at the site [2]. Treatments were randomly assigned to OTCs, thus preventing treatment effects from being confounded with spatially autocorrelated patterns, e.g., in *Phragmites* genetic relatedness or in microtopography.

Aluminum skirts at the base of each chamber (extending to 30 cm depth), in combination with low lateral movement of water at this site and the low mobility of NH_4, ensured that minimal fertilizer was removed by tidal flooding [46]. Air temperatures measured in the middle and upper *Phragmites* canopy (175 and 230 cm, respectively) in one OTC from July–October were 2.0 ± 2.8 °C (24 h mean ± SD) warmer than outside the chamber but above the native plant canopy (at 175 cm). Warming was greater during the day (3.6 ± 2.8 °C; 7:00–19:59 h) than at night (0.0 ± 0.6 °C; 20:00–6:59 h), and ∼1 °C less in the lower canopy (85 cm). This magnitude of warming is comparable to that reported for another OTC experiment at the field site [27], and is likely due to heat being trapped by both the plant canopy and by the chambers. *Phragmites* abundance within OTCs increased from 2010–2013, but the composition of most chambers in 2013 was transitional between *Phragmites*- and native-dominated. An intensive data collection effort was undertaken during the 2013 growing season to define the properties and relationships used in a simulation model of canopy growth and carbon assimilation.

2.2. GPP simulation model

We determined canopy-level carbon assimilation by combining empirical data on plant growth, canopy structure, leaf senescence, and leaf-level photosynthesis in a simulation model. Methodological details of the model structure, the empirical data we collected, and the relationships we defined from these data are provided in supplement 1; a summary is provided in table 1. Briefly, we used the R computing environment (R Foundation for Statistical Computing, Vienna, Austria) to generate virtual, monotypic stands of *Phragmites* that had characteristics of plants growing in each of the four treatments at our field site (i.e., Control, eCO_2, N_{enr}, and $eCO_2 + N_{enr}$). Empirical data from the three replicate chambers of each treatment type were pooled to determine plant characteristics in simulations.

Stand densities were established at the outset of each simulation (table 1). At daily intervals, plants grew in height (figure 1) and added leaves according to relationships derived from field data (figures S1–S3). Daily representations of *Phragmites* canopy were divided into 10 cm thick layers such that total leaf area and associated aggregate characteristics (e.g., light attenuation) could be quantified. At hourly intervals spanning the 261 days of the growing season, empirical records of light availability and air temperature were applied to the canopy. Gross carbon assimilation by each canopy layer was determined as the sum of photosynthesis and respiration rates. These were based on monthly light response curves (figure S4) recorded at the leaf level near the top of the canopy. Measured rates were adjusted to account for declines with canopy position (figure S5) as well as diurnal changes in air temperature (table 1). Adjusted rates were summed across canopy layers and through all hours of the day to yield daily GPP values (GPP_d); these were then summed through the growing season to yield GPP_a.

Phragmites stand densities vary widely in the field [16, 47, 48], and the associated changes in canopy leaf area alter carbon assimilation both positively via photosynthetic area and negatively via within-canopy shading. To assess how these countervailing processes would combine to determine carbon gain at the stand

Table 1. Simulation model components and associated properties.

Component	Property	Determination	Details
Stand	Treatment	Established at outset	Four levels: Ctrl, eCO_2, N_{enr}, $eCO_2 + N_{enr}$
	Density	Established at outset	Five levels: 50, 75, 100, 125, 150 culms m^{-2}
Culm	Height	Random draw from curve set, treatment	Logistic equation fit to weekly measurements from 113 plants (figure 1)
	Number of leaves	Culm height	Linear regression using data from 24 plants (figure S1)
Leaf	Rank	Numbered sequentially	Apical leaf = 1
	Vertical position	Leaf rank, culm height, treatment	Spline functions fit to data from 24 plants (figure S2)
	Area	Leaf rank, treatment	Means of data by leaf rank from 36 plants (figure S3)
	Living/dead	Leaf age	Constant lifespan assumed (75 d) [50]
Canopy layer	Total leaf area	Leaf area, vertical position	All leaves included (=LAI)
	Living leaf area	Leaf area, living/dead	Live leaves only
	PPFD fraction	Total leaf area	Beer's law using coefficient from [51]
	Positional correction	Treatment	Quadratic function applied to A_{net} and R_d; data from [52] (figure S5)
Carbon assimilation	Photosynthesis rate	Treatment, month, PPFD time series	A_{net} from light response curves (figure S4) based on 3 plants per chamber per month
	Respiration rate	Treatment, month	R_d from light response curves used at all PPFD
	Temperature correction	Q_{10} coefficient, temperature time series	Q_{10} values derived from [53] for photosynthesis and [54] for respiration

Note: *Determination* lists dependencies among properties and other factors used in calculations. *Details* include the datasets, functions, and other information used in calculations. A complete description of the simulation model is provided in supplement 1.

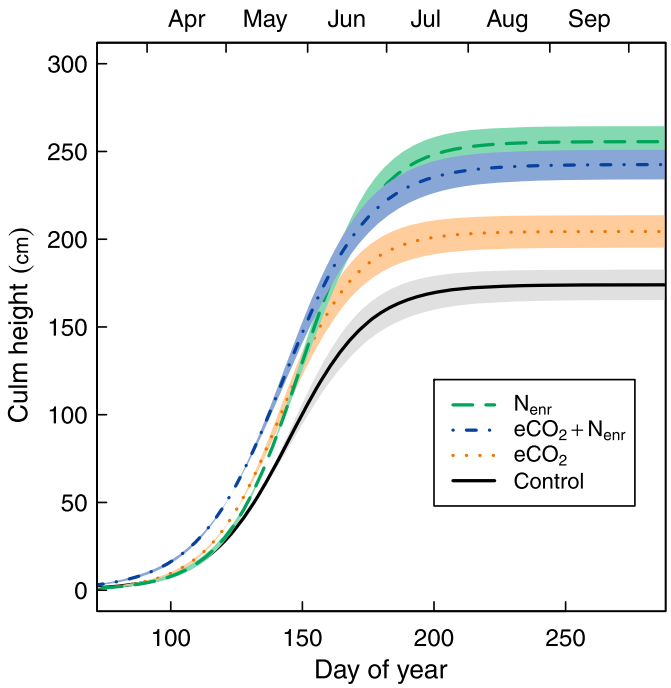

Figure 1. Mean growth curves for culm height in each of the four treatments. Lines depict the means (±1 SE) of fitted parameters from 27–29 plants per treatment being used in a logistic growth equation (see supplement 1).

scale, we ran simulations at stand densities spanning the range typically seen in Atlantic Coast marshes [16, 49]: 50, 75, 100, 125, 150 culms m^{-2}. Specifically, we ran simulations at 50, 75, 100, 125, and 150 culms m^{-2}. To characterize the influence of stochasticity associated with the selection of plant growth curves (figure 1), ten replicate model runs were carried out at each stand density. Where not stated otherwise, we report the means of replicate runs, with means computed at the daily scale. All computations were carried out in R 3.1.1.

2.3. Estimates of NPP and CUE

We calculated the NPP_a of *Phragmites* marsh under each treatment condition from estimates of aboveground biomass (BM_{ag}). Biomass was derived from

morphometric measurements on individual plants that were collected during late July 2013, near peak standing biomass; we applied allometric relationships derived from plants collected outside of the chambers to determine BM_{ag}. We then computed the mean mass per culm in each of the four treatments, and scaled these values to 100 culms m^{-2} (table S1 in supplement 2). We applied belowground mass fractions from an experiment with identical treatment levels as used in this study [55]. Note that plants in that experiment were containerized and grown from seed, potentially yielding smaller biomass allocation responses than mature plants exhibit. To convert biomass production to NPP_a, we summed above and belowground biomass estimates and assumed that plant tissue was 45% carbon by mass [56]. We calculated *Phragmites*' CUE as the ratio of NPP_a to GPP_a.

We also compared stimulation effects between GPP_a and NPP_a for *Phragmites*-dominated marsh and with NPP_a-based values for the native high-marsh community at the field site. Atmospheric CO_2 and N loading have been manipulated in factorial combination in the native marsh experiment ($n = 5$ chambers of each of the four treatment types) using identical enrichment rates to those used in the *Phragmites* study, though it began in 2005 [6]. Dominant species in the native experiment included *Schoenoplectus americanus*, *Spartina patens*, and *Distichlis spicata*, all of which produce new aboveground organs annually. Chambers were censused near peak standing biomass (late July to early August) and BM_{ag} was determined using allometric equations. Annual production of belowground biomass was measured with ingrowth bags (to 30 cm depth; collected in November). Given the low rates of decomposition in Chesapeake Bay tidal marshes [57] and the lack of dead fine roots in ingrowth bags (A Langley, personal observation), root turnover is likely to be negligible in this system. As with *Phragmites*, we assumed that biomass was 45% carbon.

3. Results

3.1. Annual carbon assimilation

Our simulations of *Phragmites australis* stands growing under current atmospheric CO_2 concentrations and ambient N conditions (i.e., the Control) yielded a GPP_a of 1.66 ± 0.05 kg C m^{-2} yr^{-1} (mean $\pm$ SD) at a typical stand density for Atlantic Coast marshes (100 culms m^{-2}; figure 2). A 300 ppm rise in CO_2 (i.e., the eCO_2 treatment) induced a 44% stimulation to GPP_a (we define stimulation as the percent increase over the Control), which equated to 2.39 ± 0.05 kg C m^{-2} yr^{-1}. Moderate N loading (i.e., the N_{enr} treatment) yielded a 60% stimulation at ambient CO_2, raising GPP_a to 2.65 ± 0.02 kg C m^{-2} yr^{-1}, while $eCO_2 + N_{enr}$ induced a 95% stimulation, raising GPP_a to 3.24 ± 0.08 kg C m^{-2} yr^{-1}. *Phragmites* culm heights, total leaf areas, and photosynthesis rates all increased under eCO_2 and N_{enr} (figures 1, S3, and S4), contributing to these effects.

Altering stand density had a curvilinear effect on GPP_a (figure 2) that was strongest under N_{enr} and weakest under the Control. Specifically, a 50% increase in stand density (from 100 to 150 culms m^{-2}) yielded increases in GPP_a of 11%–31%, while a 50% decrease in density (100 to 50 culms m^{-2}) yielded decreases in GPP_a of 27%–39%. Despite the curvilinear relationship, treatment rankings were consistent across all densities. The margins by which eCO_2 exceeded the Control (0.56–0.73 kg C m^{-2} yr^{-1}) and by which $eCO_2 + N_{enr}$ exceeded eCO_2 (0.79–0.88 kg C m^{-2} yr^{-1}) were relatively consistent (CV = 0.10 and 0.05, respectively). However, the margin by which N_{enr} exceeded eCO_2 (0.36–0.11 kg C m^{-2} yr^{-1}) decreased with stand density and was therefore more variable (CV = 0.42).

3.2. Daily carbon assimilation

Temporal patterns of carbon assimilation differed among global change scenarios, with rates on a given day strongly influenced by PPFD (figures 3(a) and (c)). GPP_d under all global change conditions exceeded rates under the Control by increasingly wide margins through most of the early growing season (March–May; figures 3(a) and (b)). Rates under N_{enr}, with or without simultaneous CO_2 addition, were greater than rates under eCO_2 through this period, and surpassed 50% stimulation through most of April and May. By the end of May, cumulative carbon assimilation represented for 17%–19% of GPP_a under the Control, eCO_2, and $eCO_2 + N_{enr}$ treatments, but 22% of annual GPP_a under N_{enr}.

During the middle of the growing season (June–July), the temporal trend in GPP_d was nearly linear under Control and eCO_2 conditions, though the rise was steeper under eCO_2 (figure 3(a)). GPP_d also increased under N_{enr}, but the trend was more variable and less steep than for the Control; rates rarely exceeded those reached in late May. Given the greater rise in GPP_d under eCO_2 than under N_{enr}, the two treatments had similar rates during the peak period of July 15–20 (34.6 ± 2.1 and 32.8 ± 1.9 g C m^{-2} d^{-1}, respectively; mean $\pm$ SD). Under $eCO_2 + N_{enr}$, the temporal trend in GPP_d paralleled that of the Control, but was 1.7× greater during the peak in mid-July (40.1 ± 2.2 versus 23.0 ± 1.3 g C m^{-2} d^{-1}).

GPP_d continued to exceed all other treatments under $eCO_2 + N_{enr}$ for the remainder of the growing season (August–November), exhibiting >100% stimulation for the majority of August and September. Carbon assimilated during the late growing season represented 27% of GPP_a under $eCO_2 + N_{enr}$. This delay in the end-of-season GPP_d decline also occurred under N_{enr}, though it was less pronounced; stimulation effects were half as strong as those under $eCO_2 + N_{enr}$ and carbon gains during the late

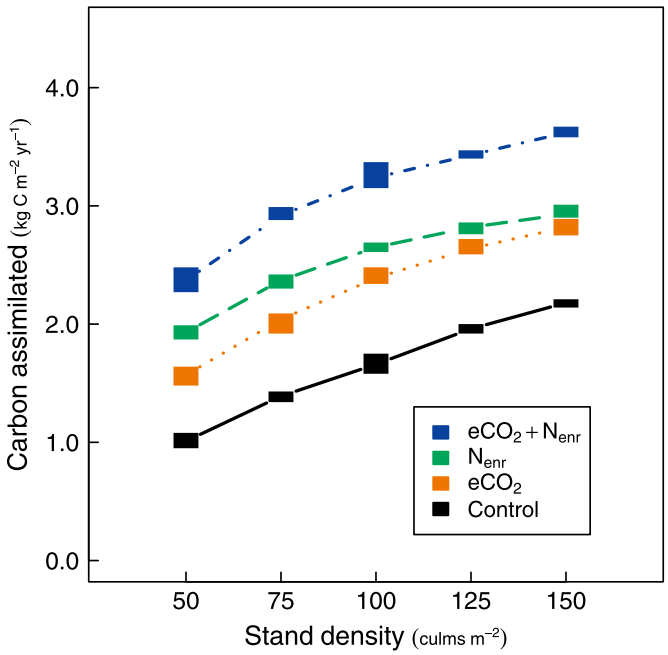

Figure 2. Annual carbon assimilation (GPP_a) by monotypic stands of *Phragmites australis* as a function of stand density. Box heights are scaled to the range of values over 10 replicate model runs, with variability resulting from the random selection of empirical height growth curves that occurred in each run.

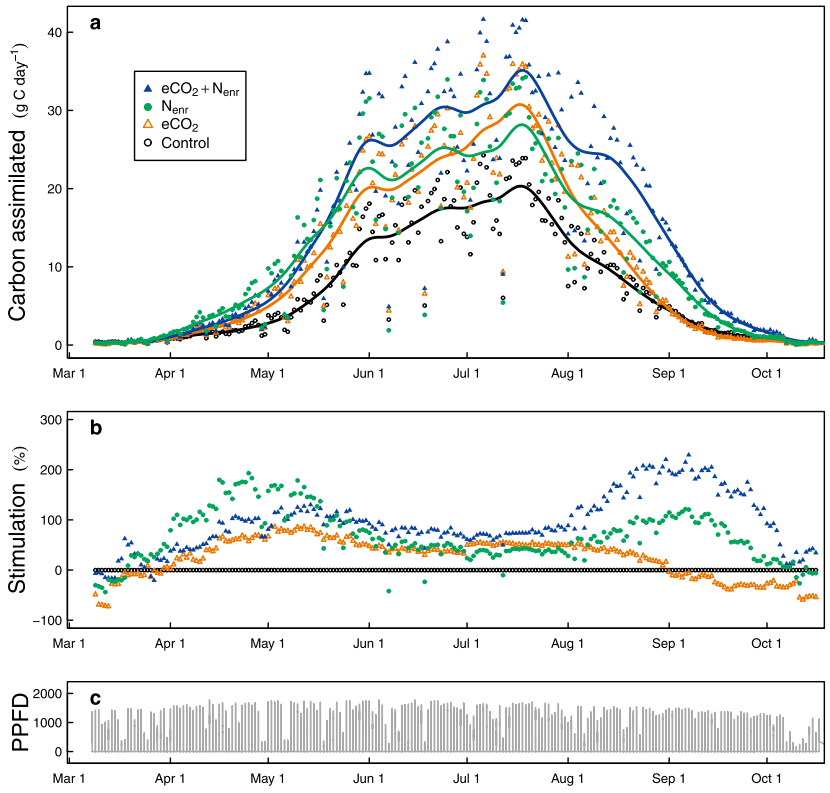

Figure 3. (a) Simulated daily carbon assimilation (GPP_d) by monotypic stands of *Phragmites australis* (100 culms m^{-2}) during the 2013 growing season. Points represent mean GPP_d rates over 10 replicate runs. Spline curves depict temporal trends for each treatment. (b) Stimulation of daily carbon assimilation by treatment, expressed as the difference from the Control on a percentage basis. (c) Daily maximum photosynthetic photon flux density (PPFD), for which units are μmol photons m^{-2} s^{-1}.

growing season accounted for 22% of GPP_a. In contrast, stimulation by eCO_2 declined throughout this period, with GPP_d rates falling below those of the Control in late August. Carbon assimilated from August–November represented 18% of GPP_a for eCO_2 and 21% for the Control.

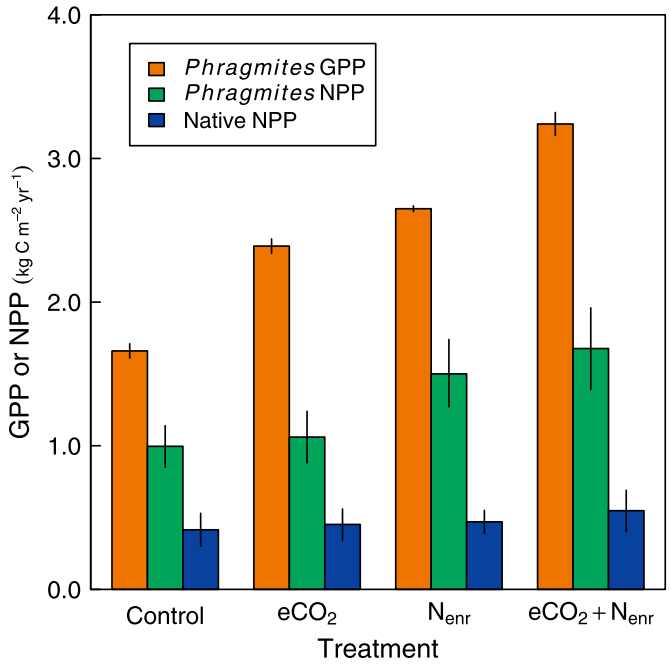

Figure 4. Primary productivity (mean ± SD) for North American mid-Atlantic coastal marshes dominated by *Phragmites australis* (100 culms m^{-2} density) or a native high-marsh plant community. Values for the *Phragmites* marsh reflect year 2013, while values for the native marsh are means over 2006–2013.

3.3. Estimates of NPP and CUE

NPP_a estimates for *Phragmites*-dominated coastal marshes ranged from 1.00–1.68 kg C m^{-2} yr^{-1}, with Control and eCO$_2$ + N$_{enr}$ conditions yielding the least and greatest rates, respectively (figure 4). NPP_a varied among treatments primarily according to their N enrichment level; this largely derived from mean aboveground biomass being similar within each N level (table S1). NPP_a was substantially greater for *Phragmites* than for the native saltmarsh community, with *Phragmites* 2.3 and 2.4× more productive than the native marsh under low N loading (i.e., Control and eCO$_2$ conditions, respectively), but 3.1 and 3.2× more productive under high N loading (N$_{enr}$ and eCO$_2$ + N$_{enr}$, respectively). Carbon retained as NPP_a represented approximately half of GPP_a for *Phragmites*, although it lost less carbon to respiration under the Control (CUE = 0.60 ± 0.09; mean ± SD, where SD was propagated from NPP_a and GPP_a) than under any global change condition; CUE was 0.44 ± 0.08 under eCO$_2$, 0.57 ± 0.09 under N$_{enr}$, and 0.52 ± 0.09 under CO$_2$ + N$_{enr}$.

Elevated CO$_2$ stimulated NPP_a in the *Phragmites* marsh far less than GPP_a (6 versus 40%, respectively), but NPP_a stimulation was similar to the multi-year average of the native marsh (9%; figure 4). N$_{enr}$ stimulated *Phragmites* GPP_a and NPP_a similarly (60 and 51%, respectively), whereas the native marsh experienced a far smaller stimulation to NPP_a (13%). The combination of eCO$_2$ + N$_{enr}$ induced the greatest stimulation effects for *Phragmites*; effects were slightly less than additive for GPP_a (95%) but more than additive for NPP_a (68%). The native marsh experienced an NPP_a stimulation under eCO$_2$ + N$_{enr}$ that was less than half of that experienced by *Phragmites* (32%).

4. Discussion

4.1. Carbon assimilation

The annual carbon assimilation computed here for monotypic *Phragmites* stands indicates that the wetlands it invades will experience a sharp increase in GPP_a under future CO$_2$ concentrations, especially where N loading is high. GPP_a is typically <2 kg C m^{-2} yr^{-1} in temperate ecosystems, including wetlands [29, 58–60], but rates can exceed that value under eutrophied conditions (e.g., 2.3 kg C m^{-2} yr^{-1} [33]). At 3.24 kg C m^{-2} yr^{-1}, the rate we computed under eCO$_2$ + N$_{enr}$ for a stand containing 100 culms m^{-2}, *Phragmites*-dominated marshes would assimilate carbon more rapidly than many other temperate ecosystems, including those measured under elevated CO$_2$ [61–63].

Our simulations indicate that changes in *Phragmites*' growth and senescence phenology are key components of its enhanced productivity under elevated N conditions, and suggest that *Phragmites* will substantially increase carbon assimilation as atmospheric CO$_2$ rises. Most notably, we observed far greater GPP_d early and late in the growing season under high versus low levels of N loading. This temporal pattern can be attributed to a combination of earlier initiation of canopy growth, prolonged canopy expansion, and maintenance of high leaf-level photosynthetic rates from June through September (figures 1, S3, S4). In

addition, *Phragmites* carbon assimilation declined late in the growing season under eCO_2. This response contrasts with that of the dominant native C_3 species at our site (*Schenoplectus americanus*), whose biomass is elevated through delays in senescence under eCO_2 [27].

4.2. Carbon retention

Under future atmospheric CO_2 concentrations, our results indicate that *Phragmites*-dominated wetlands are likely to experience stronger stimulation of NPP_a than most other wetland or upland systems. Many CO_2 enrichment studies have found small or negligible stimulation effects on productivity, especially when C_4 grasses are dominant [28, 64]. Few field studies have quantified combined $eCO_2 + N_{enr}$ stimulation effects; the three we found for grass-dominated communities that did [65–67] all based their values on current-year biomass production ($\approx NPP_a$). Stimulation effects ranged from 7 to 42% in the three studies. Similarly, the $CO_2 \times N$ experiment of the native community at the Global Change Research Wetland experienced a mean $eCO_2 + N_{enr}$ stimulation of 32% over eight years. All of these NPP_a stimulation estimates are therefore well below the 68% that we found for *Phragmites*.

Our estimates of *Phragmites*' growing season CUE (0.44–0.60) are in the middle of the range reported for wetland plant species (0.34–0.77) [33, 60, 68], suggesting that *Phragmites*' high NPP_a and strong stimulation by global change factors are due to advantages in carbon assimilation rather than an ability to minimize carbon losses via respiration. The decrease in CUE under eCO_2 relative to the Control is consistent with patterns seen in some, but not all, other studies [63]. Such decreases can arise if elevated CO_2 facilitates greater nonstructural carbohydrate production, as their metabolism can induce a greater rise in rates of respiration than photosynthesis [68]. The fertilization-induced increase in CUE seen under elevated, but not ambient, CO_2 may have been due to decreased allocation to roots causing respiration to increase less than photosynthesis [63].

4.3. Model evaluation

Results from two other studies of carbon assimilation by *Phragmites* suggest that our GPP_a values are reasonable. A study using eddy covariance reported GPP_a for a *Phragmites*-dominated marsh in northeastern China as 0.71 kg m^{-2} yr^{-1} [29]. Given that this haplotype had approximately half the maximum height (1.5 m; stand density not reported) of the *Phragmites* at our field site under ambient conditions, a GPP_a that is 52% of our modeled values for Control conditions over the range of likely stand densities (50–100 culms m^{-2}) suggests good agreement. Further, Stefanik and Mitsch [33] measured GPP for North American introduced *Phragmites* using flux chambers in a constructed freshwater wetland. Although the stand density was lower at their site than our simulation evaluated (42 culms m^{-2}; K Stefanik, *pers comm*), N loading was substantially greater ($\sim$100 g N m^{-2} yr^{-2} [69]). Nevertheless, the estimate of GPP_a in that study (3.09 kg C m^{-2} yr^{-1}) was similar to the value generated by our N_{enr} simulations at 150 culms m^{-2} (2.93 kg C m^{-2} yr^{-1}). The results of these studies demonstrate that our quantification of GPP_a is in line with values determined via more direct measurements than we used, at least under the treatment conditions considered.

Our quantification of GPP in *Phragmites*-dominated marshes had several inherent limitations. For one, we could not determine the effects of salinity, which changes inter-annually due to variation in rainfall and sea level, and reduces productivity and CO_2 stimulation effects when high [7]. Because our focal growing season had moderate salinity conditions (monthly means ranged from 8.2–12.4 ppt), years with more (or less) rainfall than occurred in 2013 would likely yield greater (or lesser) GPP_a than reported here. However, we would not expect the effect of salinity to be consistent among treatments, as elevated CO_2 is known to reduce the effects of salinity on *Phragmites* growth [70]. Second, we assumed that variables were unaffected by CO_2 and N conditions when we did not have empirical data demonstrating otherwise; these included leaf lifespan, Q_{10} values, and the decay constant for PPFD attenuation. This assumption is unlikely to hold true in many cases. For example, N enrichment can increase leaf longevity in *Phragmites* [71]. Third, although chamber temperatures reflected warming in the range expected by year 2100 [72], our temperature time series reflected contemporary conditions. If acclimation substantially altered the nature of *Phragmites*' photosynthesis response to varying temperature, our results could have been biased. However, it is difficult to predict the magnitude or direction of this potential bias, especially given that some of *Phragmites*' physiological responses to temperature are CO_2 dependent [18]. We expect to be able to address many of these limitations with empirical data once *Phragmites* densities increase in our field experiment.

5. Conclusions

The data-driven simulation of *Phragmites* canopy growth used here allowed us to translate leaf-level photosynthesis data to the stand scale, and thereby calculate GPP at a fine temporal resolution. The approach provided information on GPP that was independent of NPP measurements, making it possible to constrain CUE under global change conditions. Although the method's data requirements are not

small, similar approaches could be used in other annual systems where plant canopy structure is relatively simple. Perhaps the greatest advantage of the approach is that it can provide insight into intra-annual temporal shifts in carbon assimilation induced by global change.

By quantifying GPP at a daily resolution, we were able to determine that N enrichment sharply increased carbon assimilation both early and late in the growing season, whereas CO_2 elevation increased assimilation more moderately and through the early and mid-growing season. Given that N loading is already elevated in many North American estuaries [73], productivity advantages due to extended leaf phenology help to explain the close landscape-level association between the distribution of *Phragmites* and N enrichment [74, 75]. Our results also confirm earlier speculation that delayed leaf senescence by introduced versus native *Phragmites* in North America contributes substantially to its productivity, especially in eutrophied wetlands [56]. Further, the strong increase in late season carbon assimilation that we found under $eCO_2 + N_{enr}$ compared to N_{enr} conditions suggests that late season carbon gains will comprise an increasing fraction of *Phragmites*' annual production.

Our results indicate that *Phragmites* could increase in productivity through the coming century, given that atmospheric CO_2 levels will likely reach 700 ppm and that eutrophication will likely become increasingly widespread in that time [44, 76]. Although the productivity of native saltmarsh plants is also projected to increase in response to global change, taxa investigated previously have responded much less strongly than *Phragmites* to combined increases of CO_2 and N [6]. The plastic response to $eCO_2 + N_{enr}$ found here indicates that *Phragmites* will be able to capitalize on these two global change factors simultaneously, likely yielding stronger competitiveness than it exhibits currently. Together with other advantages that *Phragmites* gains under global change conditions, like access to deep-soil nutrients [55] and elevated patch-level genetic diversity, floret production, and therefore potential for spread via seeds [77, 78], this productivity advantage will likely translate into accelerated rates of *Phragmites* invasion in tidal marshes of the North American Atlantic Coast.

Global change-induced increases in *Phragmites* productivity may have particularly strong effects belowground. *Phragmites* allocates a substantial proportion of its growth to roots and rhizomes (82% of standing biomass in the Meadowlands of New Jersey) [79], and these penetrate more deeply into soils than do belowground organs of native plants [80, 81]. In addition to the greater root and rhizome biomass that can be expected to accompany high *Phragmites* GPP in the coming decades, belowground biomass is also likely to deepen further into the soil profile [55]. Rhizome construction costs are also lower under $eCO_2 + N_{enr}$ than under Control conditions [19], suggesting that rhizome growth could be particularly strongly enhanced under future conditions, together with rhizome-dependent processes like convective gas flow [82]. A key effect of greater rhizome and root production may be accelerated mineralization rates of sequestered nutrients, which could provide an additional N source for *Phragmites* and thereby accelerate its vegetative growth, seed production, and spread, even in sites that have low N inputs [55]. Further, exports of dissolved carbon (DOC and DIC) from wetlands invaded by *Phragmites* may increase through greater belowground productivity, potentially affecting the carbon balance of coastal aquatic communities [83].

Increases in *Phragmites* productivity also have the potential to influence carbon sequestration belowground, which determines the soil building capacity (i.e., surface accretion) of tidal wetlands, especially in peat-based systems [1]. Given rising sea levels, our estimates of NPP suggest that *Phragmites* marshes will have an increased likelihood of outpacing sea level rise than native communities [20, 84], although more refined quantifications of accretion will be needed to address this possibility with greater certainty. Coastal wetland conservation may therefore require strategic planning in order to decide whether to prevent or allow re-engineering by *Phragmites* at small spatial scales, such that ecosystem functions can be optimized at broad spatial scales. Development and refinement of predictive models like the one used here will be required to accurately forecast the local- and landscape-scale effects of global change on coastal wetland ecosystems, and to support management decisions that will mitigate the threat that accelerated sea level rise poses to their future stability.

Acknowledgments

We thank Adam Langley, Franzisca Eller, Eric Hazelton, Blanca Bernal, Joshua Shapiro, Sydne Record, several anonymous reviewers, and students in the Global Change Ecology lab at Bryn Mawr College for their valuable input on this research. We are also grateful to Gary Peresta, Andrew Peresta, and Jim Duls for maintaining the field experiment and to the SERC Phytoplankton Lab for essential data on PPFD. We thank Daniel Potts, Kay Stefanik, and Adam Langley for contributing data as well. The field experiment was funded by grants from NSF LTREB (award DEB-0950080) and Maryland Sea Grant (award SA7528114-WW). JSC was funded by a Bucher-Jackson Postdoctoral Fellowship. Additional support was provided by the Smithsonian Environmental Research Center and by Bryn Mawr College. The authors have no conflicts of interest with respect to this research.

References

[1] Kirwan M L and Megonigal J P 2013 Tidal wetland stability in the face of human impacts and sea-level rise *Nature* **504** 53–60

[2] Langley J A, Mozdzer T J, Shepard K A, Hagerty S B and Megonigal J P 2013 Tidal marsh plant responses to elevated CO_2, nitrogen fertilization, and sea level rise *Glob. Change Biol.* **19** 1495–503

[3] Langley J A and Hungate B A 2014 Plant community feedbacks and long-term ecosystem responses to multi-factored global change *AoB PLANTS* **6** plu035

[4] Craft C, Clough J, Ehman J, Joye S, Park R, Pennings S, Guo H and Machmuller M 2008 Forecasting the effects of accelerated sea-level rise on tidal marsh ecosystem services *Front. Ecol. Environ.* **7** 73–8

[5] Drake B G 2014 Rising sea level, temperature, and precipitation impact plant and ecosystem responses to elevated CO_2 on a Chesapeake Bay wetland: review of a 28-year study *Glob. Change Biol.* **20** 3329–43

[6] Langley J A and Megonigal J P 2010 Ecosystem response to elevated CO_2 levels limited by nitrogen-induced plant species shift *Nature* **466** 96–9

[7] Erickson J E, Megonigal J P, Peresta G and Drake B G 2007 Salinity and sea level mediate elevated CO_2 effects on C_3–C_4 plant interactions and tissue nitrogen in a Chesapeake Bay tidal wetland *Glob. Change Biol.* **13** 202–15

[8] McKee K L and Rooth J E 2008 Where temperate meets tropical: multi-factorial effects of elevated CO_2, nitrogen enrichment, and competition on a mangrove-salt marsh community *Glob. Change Biol.* **14** 971–84

[9] Mcleod E, Chmura G L, Bouillon S, Salm R, Björk M, Duarte C M, Lovelock C E, Schlesinger W H and Silliman B R 2011 A blueprint for blue carbon: toward an improved understanding of the role of vegetated coastal habitats in sequestering CO_2 *Front. Ecol. Environ.* **9** 552–60

[10] Orth R J *et al* 2006 A global crisis for seagrass ecosystems *Bioscience* **56** 987–96

[11] Ehrenfeld J G 2010 Ecosystem consequences of biological invasions *Annu. Rev. Ecol., Evol. Syst.* **41** 59–80

[12] Vitousek P M, D'Antonio C M, Loope L L, Rejmánek M and Westbrooks R 1997 Introduced species: a significant component of human-caused global change *N. Z. J. Ecol.* **21** 1–16 (http://newzealandecology.org/nzje/2008)

[13] Chambers R M, Meyerson L A and Saltonstall K 1999 Expansion of *Phragmites australis* into tidal wetlands of North America *Aquat. Bot.* **64** 261–73

[14] Saltonstall K 2002 Cryptic invasion by a non-native genotype of the common reed, *Phragmites australis*, into North America *Proc. Natl Acad. Sci. USA* **99** 2445–9

[15] Eller F and Brix H 2012 Different genotypes of *Phragmites australis* show distinct phenotypic plasticity in response to nutrient availability and temperature *Aquat. Bot.* **103** 89–97

[16] Mozdzer T J, Brisson J and Hazelton E L G 2013 Physiological ecology and functional traits of North American native and Eurasian introduced *Phragmites australis* lineages *AoB PLANTS* **5** plt048

[17] Mozdzer T J and Megonigal J P 2012 Jack-and-Master trait responses to elevated CO_2 and N: a comparison of native and introduced *Phragmites australis PLoS ONE* **7** e42794

[18] Eller F, Lambertini C, Nguyen L X, Achenbach L and Brix H 2013 Interactive effects of elevated temperature and CO_2 on two phylogeographically distinct clones of common reed (*Phragmites australis*) *AoB PLANTS* **5** pls051

[19] Caplan J S, Wheaton C N and Mozdzer T J 2014 Belowground advantages in construction cost facilitate a cryptic plant invasion *AoB PLANTS* **6** plu020

[20] Rooth J E, Stevenson J C and Cornwall J C 2003 Increased sediment accretion rates following invasion by *Phragmites australis*: the role of litter *Estuaries* **26** 475–83

[21] Turitzin S N and Drake B G 1981 The effect of a seasonal change in canopy structure on the photosynthetic efficiency of a salt-marsh *Oecologia* **48** 79–84

[22] Umeki K, Kikuzawa K and Sterck F J 2010 Influence of foliar phenology and shoot inclination on annual photosynthetic gain in individual beech saplings: a functional-structural modeling approach *For. Ecol. Manage.* **259** 2141–50

[23] Cleland E E, Chuine I, Menzel A, Mooney H A and Schwartz M D 2007 Shifting plant phenology in response to global change *Trends Ecol. Evol.* **22** 357–65

[24] Fridley J D 2012 Extended leaf phenology and the autumn niche in deciduous forest invasions *Nature* **485** 359–62

[25] Xia J *et al* 2015 Joint control of terrestrial gross primary productivity by plant phenology and physiology *Proc. Natl Acad. Sci. USA* **112** 2788–93

[26] Asshoff R, Zotz G and Körner C 2006 Growth and phenology of mature temperate forest trees in elevated CO_2 *Glob. Change Biol.* **12** 848–61

[27] Curtis P S, Drake B G, Leadley P W, Arp W J and Whigham D F 1989 Growth and senescence in plant communities exposed to elevated CO_2 concentrations on an estuarine marsh *Oecologia* **78** 20–6

[28] Ainsworth E A and Long S P 2005 What have we learned from 15 years of free-air CO_2 enrichment (FACE)? A meta-analytic review of the responses of photosynthesis, canopy properties and plant production to rising CO_2 *New Phytol.* **165** 351–71

[29] Han G X, Yang L Q, Yu J B, Wang G M, Mao P L and Gao Y J 2013 Environmental controls on net ecosystem CO_2 exchange over a reed (*Phragmites australis*) wetland in the Yellow River Delta, China *Estuar. Coast* **36** 401–13

[30] Schäfer K V R, Tripathee R, Artigas F, Morin T H and Bohrer G 2014 Carbon dioxide fluxes of an urban tidal marsh in the Hudson–Raritan estuary *J. Geophys. Res.: Biogeosci.* **119** 2065–81

[31] Kathilankal J C, Mozdzer T J, Fuentes J D, D'Odorico P, McGlathery K J and Zieman J C 2008 Tidal influences on carbon assimilation by a salt marsh *Environ. Res. Lett.* **3** 044010

[32] Neubauer S 2013 Ecosystem responses of a tidal freshwater marsh experiencing saltwater intrusion and altered hydrology *Estuar. Coast* **36** 491–507

[33] Stefanik K C and Mitsch W J 2014 Metabolism and methane flux of dominant macrophyte communities in created riverine wetlands using open system flow through chambers *Ecol. Eng.* **72** 67–73

[34] Anav A *et al* 2015 Spatiotemporal patterns of terrestrial gross primary production: a review *Rev. Geophys.* **53** 785–818

[35] Albaugh J M, Domec J C, Maier C A, Sucre E B, Leggett Z H and King J S 2014 Gas exchange and stand-level estimates of water use and gross primary productivity in an experimental pine and switchgrass intercrop forestry system on the Lower Coastal Plain of North Carolina, USA *Agric. For. Meteorol.* **192** 27–40

[36] Zotz G, Franke M and Woitke M 2000 Leaf phenology and seasonal carbon gain in the invasive plant, *Bunias orientalis* L. *Plant Biol.* **2** 653–8

[37] Ihm B-S, Lee J-S and Kim J-W 2004 Modelling above-ground biomass production of *Phragmites communis* Trin. stands *Ecological Issues in a Changing World* ed S-K Hong *et al* (Netherlands: Kluwer) pp 251–6

[38] Asaeda T and Karunaratne S 2000 Dynamic modeling of the growth of *Phragmites australis*: model description *Aquat. Bot.* **67** 301–18

[39] Soetaert K, Hoffmann M, Meire P, Starink M, van Oevelen D, Van Regenmortel S and Cox T J S 2004 Modeling growth and carbon allocation in two reed beds (*Phragmites australis*) in the Scheldt estuary *Aquat. Bot.* **79** 211–34

[40] Eid E M, Shaltout K H, Al-Sodany Y M, Soetaert K and Jensen K 2010 Modeling growth, carbon allocation and nutrient budgets of *Phragmites australis* in Lake Burullus, Egypt *Wetlands* **30** 240–51

[41] Allirand J M and Gosse G 1995 An above-ground biomass production model for a common reed (*Phragmites communis* Trin.) stand *Biomass Bioenergy* **9** 441–8

[42] Ondok J and Gloser J 1978 Net photosynthesis and dark respiration in a stand of *Phragmites communis* Trin. calculated by means of a model: I. Description of the model *Photosynthetica* **12** 328–36

[43] McCormick M K, Kettenring K M, Baron H M and Whigham D F 2010 Extent and reproductive mechanisms of *Phragmites australis* spread in brackish wetlands in Chesapeake Bay, Maryland (USA) *Wetlands* **30** 67–74
[44] Meinshausen M *et al* 2011 The RCP greenhouse gas concentrations and their extensions from 1765 to 2300 *Clim. Change* **109** 213–41
[45] Hopkinson C S and Giblin A E 2008 Nitrogen dynamics of coastal salt marshes *Nitrogen in the Marine Environment* ed D G Capone *et al* (San Diego: Academic) pp 991–1036
[46] Pastore M, Megonigal J P and Langley A J 2015 Elevated CO_2 promotes long-term nitrogen accumulation only in combination with nitrogen addition *Glob. Change Biol.* accepted
[47] Van der Toorn J and Mook J H 1982 The influence of environmental factors and management on stands of *Phragmites australis*: I. Effects of burning, frost and insect damage on shoot density and shoot size *J. Appl. Ecol.* **19** 477–99
[48] Warren R S, Fell P E, Grimsby J L, Buck E L, Rilling G C and Fertik R A 2001 Rates, patterns, and impacts of *Phragmites australis* expansion and effects of experimental *Phragmites* control on vegetation, macroinvertebrates, and fish within tidelands of the lower Connecticut River *Estuaries* **24** 90–107
[49] Meadows R E 2006 Aboveground competition between native and introduced *Phragmites* in two tidal marsh basins in Delaware *MS Thesis* Delaware State University
[50] Park M G and Blossey B 2008 Importance of plant traits and herbivory for invasiveness of *Phragmites australis* (Poaceae) *Am. J. Bot.* **95** 1557–68
[51] Monsi M and Saeki T 2005 On the factor light in plant communities and its importance for matter production *Ann. Bot.* **95** 549–67
[52] Hirtreiter J N and Potts D L 2012 Canopy structure, photosynthetic capacity and nitrogen distribution in adjacent mixed and monospecific stands of *Phragmites australis* and *Typha latifolia Plant Ecol.* **213** 821–9
[53] Mykleby P M, Awada T, Lenters J D, Bihmidine S, Yarina A J and Young S L J 2015 Responses of common reed (*Phragmites australis*) to nitrogen and temperature manipulations *Gt. Plains Res.* **15** 2334–463
[54] Květ J and Westlake D F 1998 Primary production in wetlands *The production Ecology of Wetlands: The IBP Synthesis* ed D F Westlake *et al* (Cambridge: Cambridge University Press) pp 78–168
[55] Mozdzer T J, Langley J A, Mueller P and Megonigal J P 2015 Deep rooting and global change facilitate the spread of an invasive grass, in review
[56] Mozdzer T J and Zieman J C 2010 Ecophysiological differences between genetic lineages facilitate the invasion of non-native *Phragmites australis* in North American Atlantic coast wetlands *J. Ecol.* **98** 451–8
[57] Kirwan M L, Langley J A, Guntenspergen G R and Megonigal J P 2013 The impact of sea-level rise on organic matter decay rates in Chesapeake Bay brackish tidal marshes *Biogeosciences* **10** 1869–76
[58] Caffrey J M 2004 Factors controlling net ecosystem metabolism in US estuaries *Estuaries* **27** 90–101
[59] Alongi D M 1998 Mangroves and salt marshes *Coastal Ecosystem Processes* (Boca Raton, FL: CRC Press) pp 43–92
[60] Rocha A V and Goulden M L 2009 Why is marsh productivity so high? New insights from eddy covariance and biomass measurements in a Typha marsh *Agric. For. Meteorol.* **149** 159–68
[61] Zhao M, Running S, Heinsch F A and Nemani R 2011 MODIS-derived terrestrial primary production *Land Remote Sensing and Global Environmental Change* ed B Ramachandran *et al* (New York: Springer) pp 635–60
[62] Falge E *et al* 2002 Seasonality of ecosystem respiration and gross primary production as derived from FLUXNET measurements *Agric. For. Meteorol.* **113** 53–74
[63] DeLucia E H, Drake J E, Thomas R B and Gonzalez-Meler M 2007 Forest carbon use efficiency: is respiration a constant fraction of gross primary production? *Glob. Change Biol.* **13** 1157–67
[64] Norby R J and Zak D R 2011 Ecological lessons from free-air CO_2 enrichment (FACE) experiments *Annu. Rev. Ecol., Evol. Syst.* **42** 181–203
[65] Reich P B, Hobbie S E and Lee T D 2014 Plant growth enhancement by elevated CO_2 eliminated by joint water and nitrogen limitation *Nat. Geosci.* **7** 920–4
[66] Schneider M K, Lüscher A, Richter M, Aeschlimann U, Hartwig U A, Blum H, Frossard E and Nösberger J 2004 Ten years of free-air CO_2 enrichment altered the mobilization of N from soil in *Lolium perenne* L. swards *Glob. Change Biol.* **10** 1377–88
[67] Dukes J S, Chiariello N R, Cleland E E, Moore L A, Shaw M R, Thayer S, Tobeck T, Mooney H A and Field C B 2005 Responses of grassland production to single and multiple global environmental changes *PLoS Biol.* **3** 1829–37
[68] Amthor J S 2000 The McCree-de Wit-Penning de Vries-Thornley respiration paradigms: 30 years later *Ann. Bot.* **86** 1–20
[69] Mitsch W J, Zhang L, Stefanik K C, Nahlik A M, Anderson C J, Bernal B, Hernandez M and Song K 2012 Creating wetlands: primary succession, water quality changes, and self-design over 15 years *Bioscience* **62** 237–50
[70] Eller F, Lambertini C, Nguyen L X and Brix H 2014 Increased invasive potential of non-native *Phragmites australis*: elevated CO_2 and temperature alleviate salinity effects on photosynthesis and growth *Glob. Change Biol.* **20** 531–43
[71] Tylová E, Teinbachová L S, Votrubová O and Gloser V 2008 Phenology and autumnal accumulation of N reserves in belowground organs of wetland helophytes *Phragmites australis* and *Glyceria maxima* affected by nutrient surplus *Environ. Exp. Bot.* **63** 28–38
[72] IPCC 2013 Summary for policymakers *Climate Change 2013: The Physical Science Basis. Contribution of Working Group I to the Fifth Assessment Report of the Intergovernmental Panel on Climate Change* ed T F Stocker *et al* (Cambridge: Cambridge University Press)
[73] Bricker S B, Longstaf B, Dennison W, Jones A, Boicourt K, Wicks C and Woerner J 2008 Effects of nutrient enrichment in the nation's estuaries: a decade of change *Harmful Algae* **8** 21–32
[74] King R S, Deluca W V, Whigham D F and Marra P P 2007 Threshold effects of coastal urbanization on *Phragmites australis* (common reed) abundance and foliar nitrogen in Chesapeake Bay *Estuar. Coast* **30** 469–81
[75] Bertness M D, Ewanchuk P J and Silliman B R 2002 Anthropogenic modification of New England salt marsh landscapes *Proc. Natl Acad. Sci. USA* **99** 1395–8
[76] Galloway J N *et al* 2004 Nitrogen cycles: past, present, and future *Biogeochemistry* **70** 153–226
[77] Kettenring K M, McCormick M K, Baron H M and Whigham D F 2011 Mechanisms of *Phragmites australis* invasion: feedbacks among genetic diversity, nutrients, and sexual reproduction *J. Appl. Ecol.* **48** 1305–13
[78] McCormick M K, Kettenring K M, Baron H M and Whigham D F 2010 Spread of invasive *Phragmites australis* in estuaries with differing degrees of development: genetic patterns, Allee effects and interpretation *J. Ecol.* **98** 1369–78
[79] Tripathee R and Schäfer K V R 2014 Above- and belowground biomass allocation in four dominant salt marsh species of the eastern United States *Wetlands* **35** 21–30
[80] Moore G E, Burdick D M, Peter C R and Keirstead D R 2012 Belowground biomass of *Phragmites australis* in coastal marshes *Northeast. Nat.* **19** 611–26
[81] Meschter J E 2015 Effects of *Phragmtes australis* (common reed) invasion on nitrogen cycling, porewater chemistry and vegetation structure in a brackish tidal marsh of the Rhode River, Maryland *MS Thesis* University of Maryland
[82] Armstrong J, Armstrong W, Beckett P M, Halder J E, Lythe S, Holt R and Sinclair A 1996 Pathways of aeration and the mechanisms and beneficial effects of humidity- and Venturi-induced convections in *Phragmites australis* (Cav.) Trin. ex Steud. *Aquat. Bot.* **54** 177–97

[83] Tzortziou M, Neale P J, Megonigal J P, Pow C L and Butterworth M 2011 Spatial gradients in dissolved carbon due to tidal marsh outwelling into a Chesapeake Bay estuary *Mar. Ecol. Prog. Ser.* **426** 41–56

[84] Langley J A, McKee K L, Cahoon D R, Cherry J A and Megonigal J P 2009 Elevated CO_2 stimulates marsh elevation gain, counterbalancing sea-level rise *Proc. Natl Acad. Sci. USA* **106** 6182–6